Technische Universiteit
Eindhoven
University of Technology

Department of Electrical Engineering

Den Dolech 2, 5612 AZ Eindhoven
P.O. Box 513, 5600 MB Eindhoven
The Netherlands
http://w3.ele.tue.nl/nl/

Series title:
Master graduation paper,
Electrical Engineering

Commissioned by Professor:
Prof. Dr. Ir. P.M.J. Van den Hof

Group / Chair:
Control Systems

Date of final presentation:
August 29, 2017

System Identification of the Inertia and Natural Damping of an Interconnected control Area

by

Author: B.J.T. Ludlage

Internal supervisors:
Prof. dr. ir. P.M.J. Van den Hof
Ir. H.H.M. Weerts

System Identification of the Inertia and Natural Damping of an Interconnected Control Area

Bernard Johann Theodor Ludlage
Department of Electrical Engineering
Eindhoven University of Technology
b.j.t.ludlage@student.tue.nl

***Abstract*— A significant increase of renewable sources, like wind and solar, in the grid has consequences for the dynamic behavior of the electric grid. The grid parameters, inertia and natural damping , will become more time-variant. Smaller values of the grid parameters result in larger and faster deviation of the frequency when a power imbalance in the grid occurs. Hence tight control of the grid frequency becomes more challenging. An up to date accurate model of the grid can help to solve this problem. Accurate models can be obtain by using dynamic network identification methods, like the Two Stage and Direct method. In this work it is investigated which methods are theoretically suitable for consistent estimation of the grid parameters and which measured signals in the grid are available for determining these parameters. The network identification is applied to estimate the grid parameters on a daily basis for two different simulation environments, a self-regulated area and an interconnected area. The grid signals are based on actual data from TenneT and E-PRICE. The results are improved by using pre-knowledge of the network and the estimation results of the previous day.**

Keywords— System identification; Dynamic network; Inertia; Damping constant; Frequency control; Power system

I. INTRODUCTION

Since the last two decades the Dutch power system is undergoing a true transformation, especially at the production side. Since the liberalization of the Dutch electricity market in 2001, the monopolistic producer per province is being replaced by a large number of competitive producers. These producers, named Balance Responsible Parties, BRP's, are each responsible for their own generation mix and obliged to help keeping the power balance in the network. Beside the conventional units like coal-fired plants, renewable sources like wind and solar become a more significant part of the generation mix. At the consumers side, demand response by incentive pricing in combination with the integration of electric vehicles is expected to become an important new aspect in the electricity market.

The power production of renewable sources is difficult to accurately predict and will continuously vary due to ever changing weather conditions. Introduction of these renewables not only influences the power generation itself, but has also consequences for the dynamic behavior of the electric grid. The inertia J and natural damping D will become more time-variant, i.e. dependent on weather conditions [2], since most renewable sources do not contribute to these grid parameters, due to the often asynchronously connection to the grid [1, 15, 16]. Another effect, which influences the damping constant, is the decrease of frequency depended load in the grid, due to the increased introduction of switch mode power convertors [2].

As a result of these changes, the dynamic behavior of the grid will become more time-variant. Smaller values of the inertia J and damping D result in larger and faster deviation of the frequency when an imbalance in the grid occurs [15]. The frequency has to be restored to its nominal value by primary and secondary control actions. Unfortunately the renewable sources do not contribute intrinsically to frequency control [2, 15]. Low level of inertia may even lead to a situation that the current frequency control is insufficient, with consequent black-outs. So the integration of more renewable sources will affect the stability of the grid and introduce future balancing challenges in the power system. Different solutions are imaginable to cope with a low level of inertia, for example faster primary control [16], control strategies based on accurate up to date dynamic models [1, 17], the introduction of battery storage systems or flywheels in the grid and even inertia markets [15].

For up to date dynamic models, it is attractive to estimate the grid parameters on-line from operational data. The inertia is often determined when a big event occurs in the grid [16]. A disadvantage of this method is that big events rarely occur in the power system. Which makes it unsuitable for estimating the continuously varying parameters. If there is sufficient excitation in the grid then system identification techniques can help to determine the accurate up to date dynamic model of a power control area. In [17], the dynamic behavior of the grid is modeled as a second order system. One of the time constants is associated with the system inertia.

In [1] the power control area is modeled in a closed loop identification framework. The presence of an autonomous excitation signal is key for the application of the used prediction error identification method to estimate the control area model [1]. The market set-point is used as autonomous signal, i.e. the market signal was used as a signal independent of the momentary load, wind power and the unknown noise sources. Note that in reality the market signal is not independent, since it is directly related to the expected load in the network, see chapter IV.

Almost all control areas in Europe are part of a large interconnected European power system. Each control area in Europe is responsible for balancing its own area. So, operators are not interested in the dynamics of the whole network, but only in the dynamics of the local control area. The European interconnected power system is an example of a dynamic

network with a known network structure. Network identification techniques, e.g. the Two-Stage and Direct method [4, 5], can be used to identify the dynamics of a particular part of the overall network, i.e. model a particular control area.

Recent developments have made network identification easier to apply in practice. There is considerable freedom in selecting the signals relevant for consistent estimation of the model dynamics [6]. The Two-Stage and Direct method have been both applied, to consistent identify the transfer function of the lumped controllable generators of one particular control area [2]. However the approach used in this paper is not applicable to determine the grid parameters.

In chapter II the problem definition and subsequent research question are defined. In chapter III the simulation model of the Dutch power system for maintaining the power balance is discussed. This model is disturbed by three external signals, wind power, load and market set-point. Chapter IV describes how to construct these external signals by using public available data of TenneT and E-PRICE. In chapter V the Dutch power system model is placed in an identification framework. Using this framework, it is determined which signals are relevant for consistent system identification and if the Two-Stage and/or Direct method are suitable to estimate the grid parameters consistent. Chapter VI gives the estimated results of the grid parameters by applying the Two-Stage method for two identical connected control areas. The estimation results of the grid parameters of a self-regulated area are described in chapter VII. Chapter VIII and chapter IX contain the conclusion and further work.

II. Problem Formulation

The grid parameters *J* and *D* need to be identified from data. For system identification it is important to have relevant independent persistently excited excitation signals available [5]. In [2], it became clear that it is not trivial to find such signals in the power grid. Most signals in the grid are insufficient informative in the frequency range of interest, or correlated to other signals, or not measurable. Moreover it is not desirable to introduce own independent sufficiently informative signals, so called probing signals, into the power system. Introduction of these additional signals will lead to a significant extra imbalance, which requires additional control action that in turn results in negative economic consequences.

In this work the electricity market is taken into account. In this liberalized market all BRP's (Balance Responsible Parties) are responsible for their own generation mix including renewable sources. This will result in additional challenges to determine the grid parameters, inertia *J* and damping constant *D* consistently. As far as the author knows dynamic network identification techniques have never been applied to estimate these grid parameters. Therefore the following problem definition and four sub-questions are defined:

Under what condition is it possible to estimate the lumped Inertia and damping parameters of a modern power system under normal operation with market mechanism and penetration of renewable sources using system identification?

1. How to set up a simulation environment, which realistically represents the dynamic frequency behavior of the 'modern' Dutch power system, as part of the European network.
2. Are there signals available in the power system which are suitable for estimation of the dynamic parameters? How are these signals characterized and what are their mutual correlations?
3. Which system identification methods are available to estimate the grid parameters *J* and *D*, assuming the presence of signals fulfilling the requirements of sub-question 2?
4. What is the accuracy of the estimated parameters achievable by the approaches developed?

The focus of this paper is to identify the grid parameters *J* and *D* of a local control area, that is part of a larger interconnected power grid, on a daily base. This work extends the previously obtained results of [1, 2] as follows: The simulations are performed with more realistic external signals as load, wind and market set point. These signals are constructed from real data obtained from the Dutch transmission system operator TenneT [11]. A different identification framework is used due the introduction of the electricity market and sample time of one second instead of four. Signals are assumed to be dependent on each other by taken into account the electricity market.

III. Power System Setup

The European power system is an interconnected system of several control areas. The Transmission System Operator (TSO) of each control area, e.g. the Dutch electricity grid, is responsible for balancing supply and demand in its own area. In this work a linear approximate simulation model is used to describe the dynamic behavior of the control area around its nominal operation point [3]. A simulation model is used because relevant data for system identification is not publicly available [11].

The simulation model in Fig. 1 is not a representation of the whole control area, but describes only the relevant parts for maintaining the power balance. The relevant parts, The Balance Responsible Parties (BRPs), the grid behavior, primary and secondary control and tie line flow, are explained in more detail in the subchapters. The model in Fig.1 contains internal signals, like frequency deviation in area 1 Δf_1, power imbalance ΔP, the secondary controller set point for BRP-j P_{Sj} and frequency deviation in area 2 Δf_2. Also external signals are available in the model, like market set point of BRP-j P_{Mj}, load P_{Load} and power production of a windmill park P_{wind}. The external signal $P_{Scheduled}$ presents the power flow over the tie line conform market agreements between the control areas. Internal signals depend of the dynamics of the system while external signals are independent of the system dynamics.

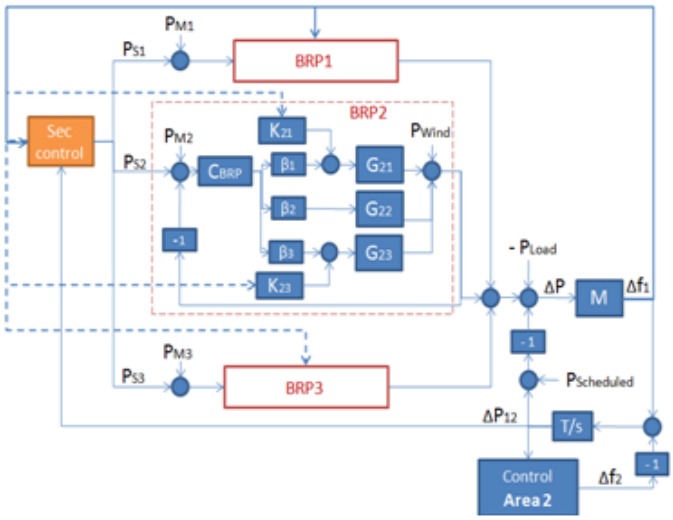

Fig. 1. Model of a control area, with three BRPs , primary and secondary control, electrical Grid (M) and connected by a tie line to control area 2 which has a frequency deviation equal to Δf_2.

A. *The Balance Resposible Parties*

The introduction of market mechanisms have resulted in several independent competing electricity producers being active in the grid. The so-called Balance Responsible Parties (BRPs) have their own generation mix. A generation mix may consist of coal fired or/and gas plants in combination with one or several renewable producers, like windmill parks or hydroelectric plants. In the control area in Fig. 1 three BRPs are active. For example BRP2 consists of three conventional plants (G_{21}, G_{22} *and* G_{23}) and a windmill park. The structure of the conventional plants is explained in more detail in appendix A. The produced power of the windmill park is modeled by the signal P_{Wind} in Fig. 1. Every BRP has its own local controller C_{BRP}, which is modeled as a I-controller. Each BRP wants to continuously achieve its power target. The controller C_{BRP} continuously adjusts the power set-point of the conventional plants to cope with deviation between the actual and the forecasted wind power of their own wind-parks. The factors β_1, β_2 and β_3 in Fig. 1 determine the distribution of the power deviation over different conventional plants.

B. *Electric Grid*

The TSO has several control mechanisms to balance consumption and production in the grid. An inequality between production and consumption is called imbalance. The imbalance is measured indirectly by measuring the frequency deviation with respect to 50Hz (the nominal frequency in Europe). This relation between power imbalance (ΔP) and frequency (Δf_1), displayed by block M in Fig. 1, depends on the total inertia J and damping constant D of the grid [3]. Block M is modeled as a first order linear system:

$$M(s) = \frac{1}{Js+D} \qquad (1)$$

C. *Primary and Secondary Control*

All BRP's specify in the market how much they want to produce for a certain time frame and price. The smallest time frame used is 15 minutes, so each day contains 96 time frames. The time frame is called a Program Time Unit (PTU). The responsibility of the market is to align production and consumption for every PTU. Controlling the imbalance during the current PTU is the responsibility of the TSO.

TenneT, the Dutch TSO, makes use of the primary and secondary controller to restore the imbalance. The primary control, also called droop control, reacts directly to limit the effect of imbalance. Since 2014, TenneT determines which plants are responsible for primary control, based on a weekly auction [12]. In Fig. 1 just two of the three plants of BRP2 take part in the primary control action. The primary control is indicated by block K in Fig. 1. All control areas take part in the primary control action, conform the ENTSO policy [10]. This introduces a tie line flow deviation ΔP_{12} between area 1 and area 2. (See appendix A for further information).

In this work the assumption is made that there is no mismatch between production and consumption in area 2. Only the imbalance in area 1 will cause a frequency deviation in area 2, Δf_2. The primary and secondary control in area 2 will respond conform the agreements of the ENTSO to the imbalance in area 1 [10].

The goal of the primary control action is to limit the frequency deviation within 30 seconds. The primary controller is a P-controller and results therefore in an small offset of the nominal frequency 50Hz. The secondary controller, an I-controller, is used to eliminate this offset in the frequency and to bring back the tie line power ΔP_{12} to zero within 15 minutes. Hence secondary control ensures that imbalance is solved in the control area where it occurs. The input of the secondary controller is frequency deviation and tie line flow, Δf_1 *and* ΔP_{12} in Fig. 1. Based on these signals and market mechanisms the secondary controller sends a set point to each BRPs, every four seconds. These set points are the signals P_{s1}, P_{s2} *and* P_{s3} in Fig. 1. Appendix A contains more detailed information about the performance of the secondary controller.

In the next chapter construction and correlation of the external signals in Fig. 1, like market P_M, load P_{Load} and wind P_{Wind}, are discussed in detail. In subchapter V.C, it will become clear why it is not necessary to construct $P_{Scheduled}$ for identification of the grid parameters J and D.

IV. Model and Signal Specification

Obtaining data for system identification in the actual control area is not trivial. The model, described in chapter III, enables simulation of signals, like frequency deviation, tie-line flow and secondary control set-points given the external signals, like wind power, load and market set-point. This chapter describes how these external signals can be constructed, based on data that has been made publicly available by TenneT and E-Price [9, 11].

The data from TenneT contains information of the forecasted and real total consumption of the Netherlands in 2009 with a one hour sampling time. The data of E-Price contains information of a part of the Dutch load consumption during a particular day of the year.

A. *Sample Time Required for Grid Parameter estimation*

The goal of the project is to estimate the grid parameters of $M(s)$, the choice of the sampling time will be determined by the dynamics of $M(s)$. In appendix A it is shown that the time constant of control area 1 equals 5.6 seconds. In order to be able to accurately estimate the model a sampling time of one second is chosen.

B. *Load Singal*

The load signal, P_{Load} in Fig. 1, represents the consumption of all Dutch consumers (industry, government and households). Unfortunately, the available data [11] has a sample time of one hour instead of the desired 1 seconds, as mentioned in IV.A. Therefore the load data is interpolated with the cubic method to one second.

This interpolated load signal contains no information about behavior of the consumers faster than an hour. The fast consumer information is added, based on an approach developed by E-PRICE[1]. A filtered white noise is therefore added to the interpolated data to represent this fast consumer behavior. The filter is a band-pass filter with cutoff frequency of $\frac{1}{60}$ and $\frac{1}{1800}$Hz and a gain of 100. This approach is also applied by E-PRICE [9].

Due to the increased use of measurement technologies, like phasor measurement units and smart meters, it is plausible to assume partial or complete knowledge of the power consumption in the future.

C. *Market Signal*

The market signal is a representation of the mean total Dutch production per PTU. Consequently the signal value changes every PTU frame. For each PTU the total production, P_{market}, is distributed over the n different BRPs:

$$P_{Market} = \sum_{j=1}^{n} P_{Mj} = a_1 P_{Market} + \ldots + a_n P_{Market}$$

with:

- $\sum_{j=1}^{n} a_j = 1$

The j-th BRP is responsible for the production of $P_{Mj} = a_j P_{Market}$. The factor a_j changes every PTU-time based on the market.

The market is responsible to align production and consumption for every PTU. So, the market set point of the total production P_{Market} is equal to the forecasted consumption $P_{Load\_Forecast}$. The database of TenneT contains information about $P_{Load\_Forecast}$ [11]. This hourly data is divided in four PTU blocks by cubic interpolation.

D. *Wind Signal*

The generation mix of the BRP2 in Fig. 1 contains one aggregated wind farm. Unfortunately the available data length in literature of a wind farms production is just one day [9]. For identification of the grid parameters the data length has to range from one day to several weeks.

Stochastic modeling is used to obtain a model, which describes the stochastic properties of wind power, to generate a realistic wind power signal over a longer time period. With the help of the identification toolbox of MATLAB, the discrete ARMA model in (2) has been created based on the data of E-PRICE[2].

$$P_{Wind\_PTU}(t) = \frac{z+0.9282}{z^3-0.6812z^2+0.0772z-0.332} w(t) \qquad (2)$$

This discrete model has a sample time of 900 seconds, corresponding to a PTU period. The power output of the ARMA model, driven by white noise with a standard deviation of 4.848, has a similar frequency spectrum as the processed data of E-PRICE, see Fig. 2.

The generated wind power data corresponds to the mean power over the PTU. The sample time becomes one second by interpolating the data (cubic interpolated method in MATLAB). This interpolated data contains no information about the fast behavior of the wind, a filtered white noise is added to simulate this high frequent behavior. The filter is a band-pass filter with cutoff frequency of $\frac{1}{90}$ and $\frac{1}{450}$. This method is also applied by E-PRICE for generating wind data with one second-interval [9].

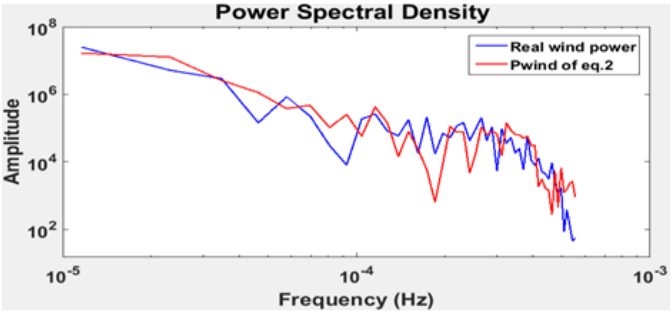

Fig. 2. The Power spectral density of the simulated $P_{Wind}(t)$ of (2) is versus the real wind farm production of a particular day obtained by E-PRICE. Remark: the frequency of $1.14 \cdot 10^{-5}$ corresponds to 1 day and the frequency of $1.1 \cdot 10^{-3}$ to 15 minutes.

V. System Identification Set-Up

In this chapter the control area in chapter III will be reformulated in a system identification framework. The thesis of Arne Dankers [4] and the papers [5, 6, 7] form the basis for the system identification framework and methods used here.

Two different methods of dynamical network identification, the Two-Stage and the Direct method [6], are evaluated whether they are suitable. The Two-Stage method requires the presence of an independent excitation signal. In theory the direct approach does not require an external excitation signal. In contrast to the Direct method, exact noise modeling is not required for the Two-Stage method.

[1] Analyzing data obtained from E-PRICE, the data reflects the consumption of a part of the Dutch society per second.

[2] The original data of E-PRICE has to be processed, because this data is interpolated with a sample time of 1 seconds. While the informative part of the data varies with 900 seconds. Therefore the original data is filtered with a low pass filter with a cutoff frequency of 1/1800 and re-sampled.

A. Dynamic Networks

A dynamic network consist of a finite set of nodes. Each node signal can be written as:

$$w_j(t) = \sum_{k \in N_j} G_{jk}^0(q) w_k(t) + r_j(t) + v_j(t) \quad (3)$$

- Set N_j contains all nodes k with a causal relation to output node j, i.e. $G_{jk}^0(q) \neq 0$. There are no self-loops, so $G_{jj}^0(q) = 0$;
- The external excitation signal r_j is known and can in some cases be freely defined;
- Signal v_j, the noise source and
- q^{-1} the delay operator, $q^{-1}u(t) = u(t-1)$.

The dynamic network can be written in a matrix notation as:

$$\begin{bmatrix} w_1 \\ w_2 \\ \vdots \\ w_L \end{bmatrix} = \begin{bmatrix} 0 & G_{12}^0 & \dots & G_{1L}^0 \\ G_{21}^0 & 0 & \dots & G_{2L}^0 \\ \vdots & \vdots & \ddots & \vdots \\ G_{L1}^0 & G_{L2}^0 & \dots & 0 \end{bmatrix} \begin{bmatrix} w_1 \\ w_2 \\ \vdots \\ w_L \end{bmatrix} + \begin{bmatrix} r_1 \\ r_2 \\ \vdots \\ r_L \end{bmatrix} + \begin{bmatrix} v_1 \\ v_2 \\ \vdots \\ v_L \end{bmatrix} \quad (4)$$

and satisfies the following assumption:

Assumption 1 [6]:

a) The network is well posed in the sense that all principal minors of $\lim_{z\to\infty}(I - G^0(z))$ are non zero.
b) $(I - G^0)^{-1}$ is stable.
c) All external excitation signals are uncorrelated with the noise signals present in the network.

The well-posedness property guarantees that both G^0 and $(I - G^0)^{-1}$ only contain proper and causal transfer functions and still allows algebraic loops.

B. The Two-Stage Method

Consider a dynamical network as defined in (4) which satisfies assumption 1. The module G_{ij}, input w_i en output w_j can be estimated consistently by the Two-Stage Algorithm 1, if the conditions of proposition 1 are satisfied. The algorithm and proposition are given below. The following sets and notations are used:

- Set D_j The internal variable(s) w_k which can serve as predictor inputs $\{w_k\}$, $k \in D_j$.
- Set P_j The external variable(s) r_k, which can serve as predictor inputs $\{r_k\}$, $k \in P_j$.
- Set T_j The external input(s) onto which will be projected $\{r_m\}$, $m \in T_j$.
- Set Z_j All internal variables which are not in the set D_j or the output variable w_j.
- θ The unknown parameters.

Algorithm 1: The Two-Stage method [6]:

1) Select w_j as the output variable to be predicted.
2) Choose the set T_j.
3) Choose the predictor input sets D_j and P_j.
4) Determine $\hat{w}_k^{(T_j)}$ for $k \in D_j$, where $\hat{w}_k^{(T_j)}$ is the projection of w_k onto all r_m, m ϵ T_j.
5) Construct the one-step-ahead predictor of w_j:

$$\hat{w}_j(t|t-1,\theta) = \sum_{k \in D_j} G_{jk}(\theta)\hat{w}_k^{(T_j)} + \sum_{k \in P_j} F_{jk}(\theta) r_k.$$

6) The parameterized transfer functions G_{jk}, $k \in D_j$ are estimated by minimizing the sum of squared (prediction) errors:

$$V_j = \frac{1}{N}\sum_{t=0}^{N-1}[w_j(t) - \hat{w}_j(t|t-1,\theta)]^2,$$

where N is the length of the data set.

The expression $\hat{w}_k^{(T_j)}$ in step 4 refers to the estimated projection of w_k onto a set of external variables $r_m, m \in T_j$, i.e. $\hat{w}_k^{(T_j)} = \sum_{m \epsilon T_j} \hat{F}_{km} r_m$ [6]. The estimated model $\hat{F}_{km}$ can be determined by using a prediction-error-method [6]. This is an open-loop-problem since r_m is assumed to be uncorrelated to all noise sources and all other external variables.

Proposition 1: Two-Stage method [6, 7]
The module G_{ji}, input node w_i and output node w_j, will be consistent estimated with the Two-Stage method (Algorithm 1) if the following conditions hold:

a) The external excitation signals $r_k \in T_j$ are uncorrelated to all $r_m \notin T_j$, except those r_m for which there is no path to w_j.
b) The set D_j satisfy the following conditions:
   1. $w_i \in D_j$ and $w_j \notin D_j$,
   2. Every path $w_i \to w_j$ goes through a node $w_k \in D_j$, excluding the path through module G_{ji},
   3. Every path $w_j \to w_j$ (loops) goes through a node $\{w_k\}$, $k \in D_j$.
c) $r_k \in P_j$, if there exist a path $r_k \to w_j$ with $k \in T_j$, which passes only through nodes in the set Z_j.
d) The parameterization is chosen flexible enough such that there exist a θ to estimate $G_{jk}(q,\theta)$ with $k \epsilon D_j$ and $F_{jk}(q,\theta)$ with $k \in P_j$ consistent.
e) The data has to be sufficiently informative, there must be at least one path from $r_m \in T_j$ to w_i.

Remark 1: There is one exception on condition b.1: The output node w_j is part of the set D_j if there exist an external excitation signal r_j at the output node. In that case condition b.3 is automatically satisfied [6].

Remark 2: Measurement noise does not influence the conditions in proposition 1, as long as the external excitation signals are exactly known [6].

C. System Identification Framework and Signal Defenition

The grid network is rewritten in a system identification framework, which can be used for consistent estimation of the grid parameters. For the sake of completeness, the identification framework is illustrated both visual and in

matrix notation. The matrix notation comply to (4). Fig. 3 is a transfer function based visualization (module-centric), commonly used in control. Each block represent a transfer function between two measurement nodes. The signals are added together by summation blocks represented as circles [5]. The transfer function to be identified is block M(s), with input node w_D and output node w_J. The nodes in Fig. 3 and matrix (5) are defined as follows:
$w_A = P_{Market} + P_{Sec}$, $w_B = P_{BRP}$, $w_C = w_A - w_B$, $w_D = \Delta P$, $w_E = P_{Tie}$, $w_F = \Delta f_{12}$ and $w_J = \Delta f_1$ resulting in:

$$\begin{bmatrix} w_A \\ w_B \\ w_C \\ w_D \\ w_E \\ w_F \\ w_J \end{bmatrix} = \begin{bmatrix} 0 & 0 & 0 & 0 & G_{AE} & 0 & G_{AJ} \\ 0 & 0 & G_{BC} & 0 & 0 & 0 & G_{BJ} \\ 1 & -1 & 0 & 0 & 0 & 0 & 0 \\ 0 & 1 & 0 & 0 & 1 & 0 & 0 \\ 0 & 0 & 0 & 0 & 0 & G_{EF} & 0 \\ 0 & 0 & 0 & 0 & -X & 1 & 0 \\ 0 & 0 & 0 & M & 0 & 0 & 0 \end{bmatrix} \begin{bmatrix} w_A \\ w_B \\ w_C \\ w_D \\ w_E \\ w_F \\ w_J \end{bmatrix}$$

$$+ \begin{bmatrix} P_{Market} \\ P_{Wind\_Forecast} \\ 0 \\ -P_{Load\_Forecast} \\ P_{Scheduled} \\ 0 \\ 0 \end{bmatrix} + \begin{bmatrix} 0 \\ V_{Wind} \\ 0 \\ -V_{Load} \\ 0 \\ 0 \\ 0 \end{bmatrix}. \qquad (5)$$

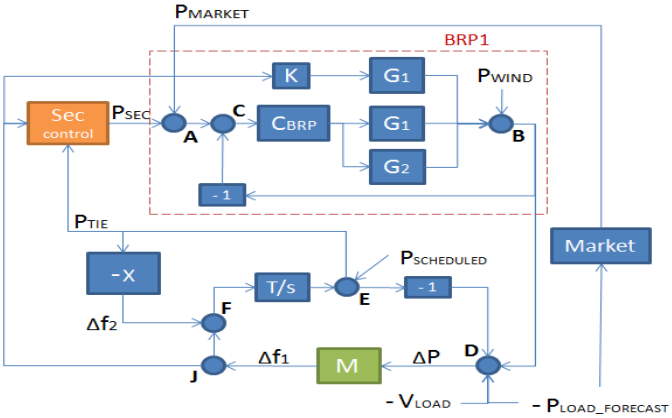

Fig. 3. System Identification framework of control area 1.

Below the identification framework nodes and external signals from (5) and Fig. 3 are defined. This information is relevant to determine the predictor input sets, chapter V.D and V.E.

The market sends every PTU (15 minutes) a set-point to the BRPs, P_{Market}. In fact the market signal is not only determined by the forecasted load as mentioned in chapter III, but also by $P_{scheduled}$,

$$P_{Market}(t) = P_{Load\_Forecast}(t) - P_{Scheduled}(t). \qquad (6)$$

The signal $P_{scheduled}$ presents the power flow over the tie line conform market agreements between the control areas and is part of the tie line flow $P_{Tie}(t)$,

$$P_{Tie}(t) = \Delta P_{12}(t) + P_{Scheduled}(t). \qquad (7)$$

In this study $P_{scheduled} = 0$, because it is unsuited as an external excitation signal, since it is related to $P_{Load\_Forecast}$ and P_{Market}, see (6) and condition (a) of proposition 1.
So, the total production P_{market} is equal to the total forecasted load $P_{Load\_Forecast}$. Therefore the signal $P_{Load\_Forecast}$ enters the system at two different places in Fig. 3, with a positive sign at node w_A and a negative sign at node w_D.

The forecasted wind power, $P_{Wind\_Forecast}$, determines the market position of a BRP with a wind farm in its generation mix. So, the forecasted wind is part of the overall production of this BRP. The BRP will respond to deviation between the actual and forecasted power production of its wind farms, V_{Wind}, by adjusting the set-points of its own conventional power units.

The difference between the actual Dutch consumption, P_{Load} and the forecasted load, $P_{Load\_Forecast}$ can be defined as

$$V_{Load}(t) = P_{Load}(t) - P_{Load_{Forecast}}(t). \qquad (8)$$

The signal V_{Load} can be determined continuously by using the signals P_{Load} and $P_{Load\_Forecast}$ as defined in chapter IV. So, the real time V_{Load} is assumed to be known.

The values of the nodes w_A, w_E, w_J and w_F in (5) are available at a sampling rate of one second. The $P_{Tie} = \Delta P_{12}$ and Δf_1 are measured every second for a proper secondary control. The secondary controller signal, P_{sec}, is a ZOH signal which changes every four seconds, see appendix A. Node w_F is the difference in frequency of the two control areas, $\Delta f_{12} = \Delta f_1 - \Delta f_2$. Control area 2 exchanges information to area 1 of the measured values of Δf_2 with a sample rate of one second.

Node w_D represents the imbalance of area 1 and can be expressed as, $\Delta P = P_{BRP} - P_{Load\_Forcast} - V_{Load} - \Delta P_{12}$. Nodes w_B, w_C and w_D in (5) depend of the BRP's production. Due to market technical reasons [12], only the average BRP production during a PTU (15 minutes) is published. These nodes have a sample rate of 15 minutes.

Block X is essential for satisfying assumption 1.C. Although Δf_2 is measurable, this signal cannot be considered as external excitation or measurable noise signal, because it is direct related to the noise sources V_{Load} *en* V_{wind}.

D. Define set D_J

The system identification framework in Fig. 3 is used as starting point for determining the internal variable which are part of the predictor input set D_J. The set D_J must fulfill the conditions of proposition 1.b and all w_k, $k \in D_j$, have a sample rate of one second. The last requirement is important for estimating the grid parameters (sub chapter IV.A).

According to proposition 1.b, the input variable of the estimated model M, w_D, is part of the predictor input set D_J. This leads to a problem, because node w_D also depends on the BRP production, which is only known as an average over the total PTU. Hence the real power imbalance at node w_D is not available at a sample rate of one second.

A solution is to split node w_D in a part known at a sample rate of one second and part that is unknown at this sampling rate, say node w_{Db} respectively node w_{Do}. Node w_{Db} contains the signals with a sample rate of one second, i.e. ΔP_{12} and

V_{Load}. This makes the input node w_{Db} suitable to be part of the set D_J. Node w_{Do} consist of the signals $P_{Load\_Forecast}$ and P_{BRP} that are unknown at a sampling rate of 1 Hz. The signal $P_{Load\_Forecast}$ enters the system at node w_A and w_{Do}. As the dynamic relation between node w_A and w_{Do} is fast and has steady state gain of one, the node w_{Do} contains only a high-pass filtered version of P_{market}. As the signal is high frequent and of small amplitude, it is considered as an unknown noise term at node w_{Do}.

Splitting node w_D requires a restructuring of the network topology in Fig. 3. This restructuring is illustrated in Fig. 4. As a consequence a new loop is created, $w_J \rightarrow w_B \rightarrow w_{Do} \rightarrow w_J$. This loop contains the unknown nodes w_B and w_{Do}. Therefore these nodes are not suitable to be part of the set D_J and the third condition for defining set D_J cannot be satisfied.

Remark 3: It is not possible to make output node w_J part of the set D_J, because of the absence of any external excitation signals at node w_J (remark 1 sub chapter V.B).

This problem can be solved by using the properties of the network structure. There is a direct connection between node w_J and w_F with known dynamics. This makes w_F also a suitable output node of block M.

The choice of output node w_F as output node, makes it necessary to restructure the network topology, which are illustrated in Fig. 4. Instead of the path $w_{Db} \rightarrow w_J \rightarrow w_F$, there is a direct path between node w_{Db} and node w_F. The same adjustment is made at node w_{Do}, to maintain the network behavior.

The sets in the introduction of chapter V are renamed, because a 'new' output node w_F: D_F, Z_F, P_F, T_F has been defined. Defining node w_F as output node makes it possible to construct the predictor input set: $D_F = \{w_{Db}, w_J, w_E\}$ and $Z_F = \{w_A, w_B, w_C, w_{Do}\}$. Due to the parallel paths $w_{Db} \rightarrow w_J \rightarrow w_A \rightarrow w_B \rightarrow w_{Do} \rightarrow w_F$ and $w_{Db} \rightarrow w_J \rightarrow w_B \rightarrow w_{Do} \rightarrow w_F$, node w_J is part of the predictor input set. While node w_E is part of all output loops. So, the set $D_F = \{w_{Db}, w_J, w_E\}$ satisfies the condition of proposition 1.b.

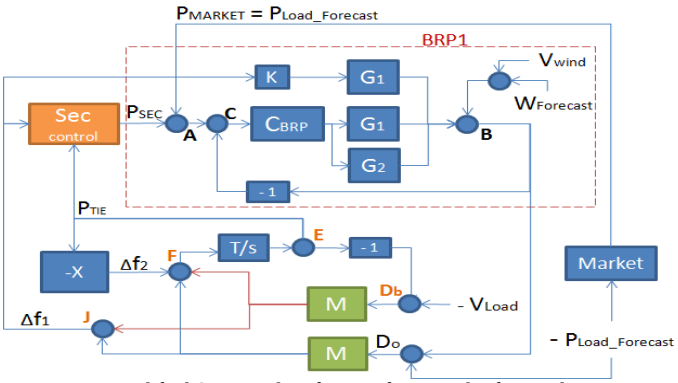

Fig. 4. Modified System Identification framework of control area 1.

E. Define Set T_F and P_F

The identification framework in Fig. 4 is used to determine the sets T_F and P_F. For the Two-Stage method it is crucial that there is an suitable external excitation signal available, i.e. that the set T_F needs to be nonempty. From Fig. 4, the following possible external excitation signals are available: $P_{Load\_Forecast}$, $P_{Wind\_Forecast}$ and V_{Load}.

The external signal must be uncorrelated to all other signals, according condition (a) proposition 1, to be part of the set T_F. The signal $P_{Load\_Forecast}$ enters the system at two different positions in Fig. 4; positive at node w_A (production) and negative at node w_D (consumption). As these external signals are correlated they cannot be part of the set T_F conform condition (a) of proposition 1. Also, the signal $P_{Wind\_Forecast}$ cannot be part of the set T_F because it is directly related to the market position of the BRP.

The last remaining external signal V_{Load} (8) enters the network via the node w_{Db} and is independent of all previously mentioned signals. Hence it fulfills condition (a) of proposition 1 and $T_F = \{V_{Load}\}$. The set $P_F = \{\emptyset\}$, because V_{Load} passes through a node in the set D_F, namely node w_{Db}, see proposition 1.c.

As discussed in chapter III, more than just one BRPs is responsible for maintaining balance. The ID framework however contains just one BRP, which represents all the BRPs. For the system identification method, it is irrelevant if there are one or more BRPs present.

Note that the BRP related nodes, node w_A, w_B and w_C are not part of the predictor input sets.

F. Including Pre-knowledge in the set

As the secondary controller contains an integrator the power spectra of node signals w_E and w_J, as they are the inputs for this integrator, will be high-pass filtered signals, which results in poor signal to noise ratios at lower frequencies. In order to improve the signal to noise ratio in this frequency range one can make use of this structural knowledge on the integrator and integrate the signals w_E and w_J before identifying the system. This results in the new predictor input set: $D_F = \left\{w_{Db}, \frac{1}{s}w_E, \frac{1}{s}w_J\right\}$. Applying this pre-knowledge on the integrator will turn out to improve significantly the identification results, see next chapter.

G. Direct Method

The Direct method uses the same predictor input sets (D_F, P_F) as defined for the Two-Stage method in subchapter V.C and V.D [6]. The network topology in Fig. 4 is therefore also suitable for the Direct method. The grid parameters in block M, with input w_{Db} and output w_F, can be determined consistent with the Direct method if all conditions in proposition 7 of article [6] are satisfied. One of those conditions is the absence of a confounding variable (definition 1).

Definition 1 [6]:
Consider the output variable w_F and set D_F of the predictor inputs. A variable, v_L, is a confounding variable if both conditions hold:

a) There is a path from v_L to w_F that passes only through $w_{m,}m \in Z_F$.
b) There is a path from v_L to $w_k, k \in D_F$ that passes only through $w_{m,}m \in Z_F$.

The node w_{Do}, which is part of the set Z_F, is influenced by the high frequent filtered P_{Market} noise term. This noise term directly influences both the predictor input node w_J as the output node w_F, see Fig. 4. Therefore the high frequent filtered P_{Market} signal is a confounding variable and hence the Direct method cannot be used.

VI. Simulation Results Two connected Areas

In the previous chapter, it has been shown that it is theoretically possible to estimate the grid parameters J and D consistently with the Two-Stage method. In this section, it is investigate how accurate these parameters can be determined in practice.

In the next set of experiments the parameters are estimated on a daily base for the period 2 until 7 September. Monday 1 September is excluded due to transient effects. Beside the external excitation signal, V_{Load}, also the terms $P_{market,}\, P_{wind,}\ \ P_{Load\_forecasted}$ in area 1 are taken into account. In chapter IV and V.C is described how these signals are constructed by using the relevant data of TenneT and E-PRICE. As mentioned in chapter III, there is no mismatch between consumption and production in control area 2, i.e. $P_{market\_A2} = P_{Load\_A2} = 0$.

The two control areas in the simulation framework of Fig. 4 are assumed to be identical. This framework is used in chapter V to illustrate that consistent estimation is possible with the Two-Stage method. In this framework, w_F is the output and w_{Db} the input node of the estimated first order block $M(s)$ with the following predictor input sets: $D_F = \left\{w_{Db}, \frac{1}{s}w_E, \frac{1}{s}w_J\right\}$, $T_F = \{V_{Load}\}$ and $P_F = \{\emptyset\}$.

This information corresponds with step 1-3 of the Two-Stage Algorithm 1. The generated discrete node data w_J, w_E and w_{Db} is a ZOH-signal with a sample time of one second. In step 4 of Algorithm 1, the influences of the external excitation signal V_{Load} at the three predictor input nodes is estimated, i.e. $\widehat{w}_{Db}{}^{(V_{Load})}, \widehat{w}_E{}^{(V_{Load})}$ and $\widehat{w}_J{}^{(V_{Load})}$. This results in three open loop SISO problems.

The models, $\hat{F}_{Db\_Vload}$, $\hat{F}_{Db\_Vload}$ and $\hat{F}_{Db\_Vload}$ are estimated by using the option Transfer Function Model in the System Identification Toolbox in MATLAB. The order of the models are determined on experience, zero/pole cancellation and the resulting step response. These three models are then used to estimate the effect of the excitation signal V_{Load} at the three predictor input nodes $\widehat{w}_{Db}{}^{(V_{Load})}$, $\widehat{w}_E{}^{(V_{Load})}$ and $\widehat{w}_J{}^{(V_{Load})}$. Fig. 5 shows the cross-correlation of the signal V_{Load} and ε_{DB} at Tuesday, whereby $\varepsilon_{DB} = w_{Db} - \widehat{w}_{Db}{}^{(V_{Load})}$. The low cross-correlation indicates that the projection of $\widehat{w}_{Db}{}^{(V_{Load})}$ is estimated well. From Fig. 5 it can be also concluded that the projections $\widehat{w}_E{}^{(V_{Load})}$ and $\widehat{w}_J{}^{(V_{Load})}$ are estimated well.

The order of the estimated models in step 4 are given in Table 1. For example the transfer function $\hat{F}_{E\_Vload}$ at Tuesday has three poles and three zeros, indicated by [3 3] in Table 1.

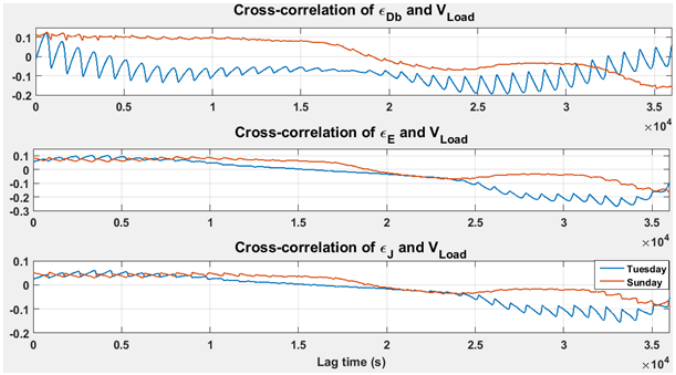

Fig. 5. The cross-correlation of the signals $\varepsilon_{DB}, \varepsilon_J, \varepsilon_E$ and V_{Load} for Tuesday 2 September (blue) and Sunday 7 September (red).

For the next step, pre-knowledge on the network structure is used to improve the estimation results. The projections $\widehat{w}_E{}^{(V_{Load})}$ and $\widehat{w}_J{}^{(V_{Load})}$ from step 4 are integrated, conform section V.F. In step 5 and 6 of Algorithm 1, the dynamics between the projections, $\widehat{w}_{Db}{}^{(V_{Load})}, \frac{1}{s}\widehat{w}_E{}^{(V_{Load})}$ and $\frac{1}{s}\widehat{w}_J{}^{(V_{Load})}$, and the output w_F are estimated with the option continuous time process models using the identification toolbox in MATLAB. These low order models are popular in the industry and describes the system dynamics using static gain and characteristic time constant associated with poles and zeros [8]. Solving this MISO open-loop problem lead to the desired grid parameters J and D.

The following three open-loops path have to be estimated:

$$\widehat{w}_{Db}{}^{(V_{Load})} \rightarrow w_F$$
$$\frac{1}{s}\widehat{w}_E{}^{(V_{Load})} \rightarrow w_A \rightarrow w_B \rightarrow w_{Do} \rightarrow w_F$$
$$\frac{1}{s}\widehat{w}_J{}^{(V_{Load})} \rightarrow w_A \rightarrow w_B \rightarrow w_{Do} \rightarrow w_F$$

From above and Fig. 4, it can be concluded that all paths contain block M. The settling time between node w_A and w_B is two seconds. Compare to block M, with a settling time of 30 seconds, the transfer between node w_A and w_B is negligible and therefore equal to 1. So, three first order models have to be estimated.

The grid parameters J and D are estimated well for Tuesday, see Table 1. The percentages in Table 1 indicate the deviation from the original grid values($J = 2.0,\ D = 0.358$). For each further day, the results of the previous day are used as initial guess in step 6 of Algorithm 1 to try to prevent converging to a local minimum of the non-linear cost function used in the identification.

From Table 1 it is observed that the parameters are estimated well for most of the days with the Two-Stage method. For these days, the maximum estimation error is just 2.5%. In the weekend, especially the Sunday, the results are less reliable. The D_{est} at Sunday corresponds with 108.4% of the original value while the inertia estimation error is 7%.

TABLE I
Identification results of block M(s) for two identical connected control areas, for the period 2-7 September 2009.

Day	J_{est}	D_{est}	F_{Db_VLoad}	F_{E_VLoad}	F_{J_VLoad}
Tue	2.00 (0.0%)	0.361 (0.8%)	[1 0]	[3 3]	[4 3]
Wed	2.00 (0.0%)	0.355 (0.8%)	[3 2]	[3 3]	[4 3]
Thu	2.02 (1.0%)	0.353 (1.4%)	[1 0]	[3 3]	[4 3]
Fri	2.05 (2.5%)	0.350 (2.2%)	[1 0]	[4 3]	[4 3]
Sat	2.05 (2.5%)	0.388 (8.4%)	[3 2]	[4 3]	[4 3]
Sun	1.86 (7.0%)	0.388 (8.4%)	[2 1]	[4 3]	[4 3]

In Fig. 5, the cross-correlations of ε_{DB} and V_{Load}, ε_E and V_{Load} and ε_J and V_{Load} for Sunday 7 September are plotted in red. It can be concluded that the SISO open-loop problems of step 4 of Algorithm 1 are solved well. Moreover the models obtained from the second step correspond to the ones found on the other days. It is therefore expected that something goes wrong in the second estimation (step 5 and 6 of Algorithm 1). A possible cause can be found in the correlation between the estimated projections or due to an insufficient excitation of the external excitation signal. Further research is recommended.

Remark: The identification results of period 8-15 September in table B.1 in appendix B support the results of week 1. The model for the Sunday of week 2 is again very inaccurate. Despite of a wrong initial model from Sunday, the model for the Monday in week 3 is estimated well again (table B.1).

VII. Self-Regulated Area

A self-regulated country, for example Cyprus or Kreta, is not connected to other control areas and responsible for its own frequency control. Fig. 6 illustrates the identification framework of a self-regulated country. Compared to the identification framework of the two connected control areas in Fig. 4, the nodes w_E and w_F are not considered, since the transfer function X is not present. For this scenario, node w_J is the output of the estimated model, see Fig. 6. In accordance with proposition 1 in chapter V, the following predictor input sets are defined for a self-regulated area: $D_J = \{w_{Db}, \frac{1}{s}w_J\}$, $T_J = \{V_{Load}\}$ and $P_j = \{\emptyset\}$. This information corresponds with step 1 till 3 of Algorithm 1.

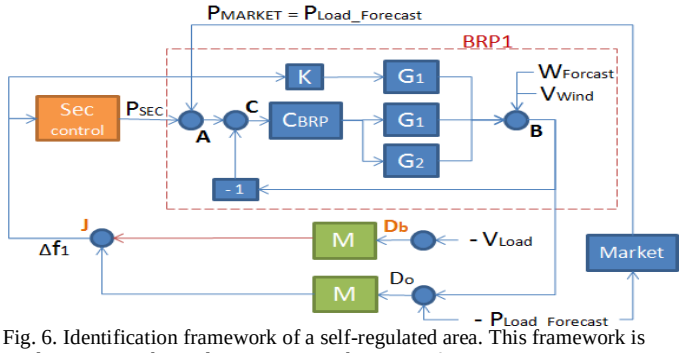

Fig. 6. Identification framework of a self-regulated area. This framework is used to estimate the grid parameters in chapter VI.A.

The whole power system of the self regulating country is taken into account. This means the availability of V_{Load} and the market related signals $P_{market,}$ $P_{wind,}$ $P_{Load\_forecasted}$ in the grid. These signals are constructed based on the data from TENNET as discussed in chapter IV.

The simulated signals, w_{Db} and w_J have a sample time of 1 second and are considered as a ZOH-signals. The estimation methods of step 4, 5 and 6 of Algorithm 1 are similar as described for the two connected areas. In step 4 of Algorithm 1, two open-loop problems have to be solved. From Fig. 6, the open-loop transfer between V_{Load} and node w_{Db} is equal to 1, i.e. $\hat{F}_{Db\_Vload} = 1$. The best estimation results of the grid parameters are obtained when $\hat{F}_{J\_Vload}$ has three poles and two zeros. Whereby one of the zeros is a differentiator. The dynamic behavior of the estimated model $\hat{F}_{J\_Vload}$ is similar for each day, except Sunday.

In step 5 and 6 of Algorithm 1, the dynamics between the projections, $\hat{w}_{Db}{}^{(V_{Load})}$ and $\frac{1}{s}\hat{w}_J{}^{(V_{Load})}$ and the output w_J are estimated. Solving this MISO open-loop problem lead to the desired grid parameters J and D. In Table C.1 in appendix C, the estimation results are shown for the period 2-7 September. At Tuesday the damping constant D has a estimation error of 4% and the inertia J even 25%. As is seen from the correlations of the normalized signals in Fig. 7, the disappointing accuracy of the estimation is a direct consequence of the dependency between the signals $\hat{w}_{Db}{}^{(V_{Load})}$ and $\frac{1}{s}\hat{w}_J{}^{(V_{Load})}$. As the goal of the secondary I controller is to bring the frequency back to zero, i.e. make the power imbalance zero, the P_{Sec} will follow V_{Load} (see Fig. 6). Hence a tightly tuned secondary control will result in a dependency between $\hat{w}_{Db}{}^{(V_{Load})}$ and $\frac{1}{s}\hat{w}_J{}^{(V_{Load})}$.

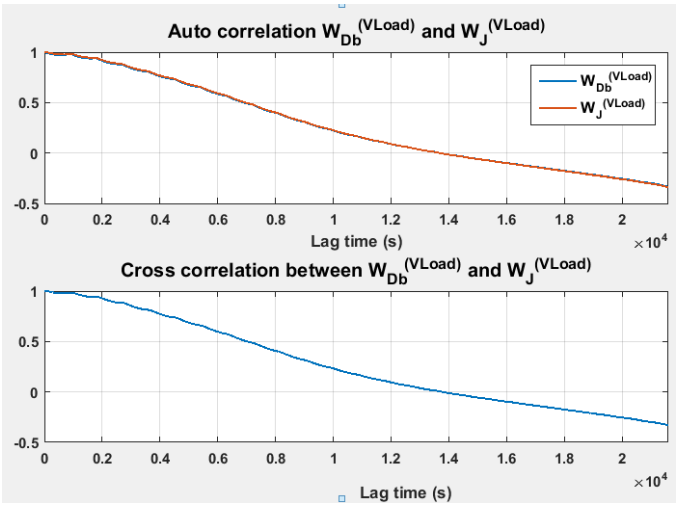

Fig. 7. Auto correlation of the estimated projections $\hat{w}_{Db}{}^{(V_{Load})}$ and $\frac{1}{s}\hat{w}_J{}^{(V_{Load})}$ at Tuesday. The bottom plot shows the cross correlation between both projections.

VIII. Conclusion

The estimating results of the parameters J and D with the two stage method are promising for two connected control areas. This corresponds with the reality, most European control areas are connected to one or several control areas.

For consistent estimation the following predictor input sets are used $D_F = \{w_{DB}, w_E, w_J\}$ and $T_F = \{V_{Load}\}$ and output node w_F. I.e. the following measurable signals in the grid are relevant: frequency deviation area 1 (Δf_1) and area 2 (Δf_2), tie line flow deviation (ΔP_{12}) and load error (V_{Load}).

There are two ways to improve the estimation results: Using pre-knowledge of the network, the paths between the output node w_F and input nodes w_E and w_J contain both an integrator (secondary controller). Before identifying the parameters, the nodes w_E and w_J are integrated. This improved the low frequency power content of these signals drastically. Secondly, the results of the previous day are used as initial guess in step 6 of Algorithm 1 to try to prevent converging to a local minimum of the non-linear cost function used in the identification.

For the two identical connected control areas, the estimation results for the weekdays differs less than 2.5% of the real grid values. Compare to the weekdays, the results of the weekend days are worse, especially at Sunday. The models obtained from the second step at Sunday correspond to the ones found on the weekdays. It is therefore expected that something goes wrong in the second estimation (step 5 and 6 of Algorithm 1). A possible cause can be found in the correlation between the estimated projections or due to an insufficient excitation of the external excitation signal. Further research is recommended.

The estimation results are the same for each day of the week in case of a self-regulated area. Unfortunately, there is a bias term, the damping constant D has a estimation error of 4% and the inertia J even 25%. The disappointing accuracy of the estimation is a direct consequence of the dependency between the signals $\widehat{w}_{Db}{}^{(V_{Load})}$ and $\frac{1}{S}\widehat{w}_J{}^{(V_{Load})}$.

The Direct method is unsuitable for consistent estimating of the grid parameters, due to the presence of confounding variable in the identification framework.

IX. Future Work

The original data of TenneT for the market related signals, P_{Market} and P_{Load}, have a sample time of one hour. These signals are relevant to create the external excitation signal V_{Load}. In this paper the data is interpolated to a sample time of one second, based on a limited understanding of the behavior faster than 1 hour. The one second sampling time is necessary for identification of the parameters J and D. The help of TenneT is required to obtain more realistic data with a sample time of one second.

In this paper it is assumed that there is no mismatch between production and consumption in area 2. Only the imbalance in area 1 will cause a frequency deviation in area 2, Δf_2. This does not correspond with the reality. The mismatch between production and consumption in area 2, act as a non-measurable disturbance and will influences the output node w_F and the predictor input set. Further investigation is required to obtain insight impact of this non-measurable disturbance on the estimation of the parameters in area 1. Moreover the larger the relative size of the neighboring control area the more effect it is expected to have on the estimation of the parameters in control area 1.

In Europe there is a trend to increase the number of connections between control areas. This has no theoretical consequences for the mentioned identification method in chapter V. The tie-line flows of all connections can always be centered in node E, appendix D.

The predictor input set and method will not change if the control area is connected to multiple control areas. The tie line flow deviation between area 1 and 3, ΔP_{13}, is a measurable disturbance, and therefore part of the 'known' node Db. In appendix D the system identification framework is given for control area connected to two other areas.

For proper estimation using the Two-Stage method it is important that the relevant subsystems are linear. In practice non-linearities are present in the grid [2]. More research is required to get a detailed understanding of the impact the non-linearities have on the accuracy of the results obtained by the two stage method.

References

[1] A. Virag, A. Jokic, P.P.J. van den Bosch and P.M.J. Van den Hof, "Using market schedules to improve secondary control design," IEEE

[2] H.D.J. Laurijsse, "System Identification of Individual Control Area Dynamics in Interconnected Power systems," Master graduating paper, Eindhoven University of Technology, 2014.

[3] P. Kundur, *Power System Stability and Control*, McGraw-Hill, Inc., 1994.

[4] A. Dankers, "System Identification in dynamic networks," Ph.D. dissertation, Delft University of Technology, 2014.

[5] P.M.J. Van den Hof , A. Dankers, P.S.C. Heuberger, X. Bombois, "Identification of dynamic models in complex networks with prediction error methods__Basic methods for consistent module estimates," *Automatic*, vol.49, pp. 2994-3006, Oct. 2013.

[6] P.M.J. Van den Hof , A. Dankers, P.S.C. Heuberger, X. Bombois, "Identification of Dynamic Models in Complex Networks With Prediction Error Methods: Predictor Input Selection," *IEEE Trans. Autom. Control*., vol. 61, no. 4, pp 937-952, 2016.

[7] P.M.J. Van den Hof , A. Dankers, P.S.C. Heuberger, X. Bombois, "Predictor input selection for two stage identification in dynamic networks," *in Proc. ECC*, Zurich, Switzerland, Jul. 2013, pp. 1422-1427.

[8] L. Ljung, "System Identification Toolbox™ User's Guide", The MathWorks, R2015a.

[9] Data Eprice – WP6 Results: http://www.e-price-project.eu/website/TLL/eprice.php?OPId=15

[10] European Network of Transmission System Operators for Electricity (ENTSO-E), "Operation Handbook, Policy 1, Load-Frequency Control and Performance," Tech. Rep. Cc, 2009. Online: https://www.entsoe.eu/publications/system-operations-reports/operation-handbook

[11] Data TenneT: http://energieinfo.tennet.org/Consumption/RealisedConsumption.aspx.

[12] Systeemcode elektriciteit, kenmerk ACM/DE/2016/202152, Autoriteit consument en markt (ACM), 17/03/2017. Online: http://wetten.overheid.nl/BWBR0037947/2017-03-17.

[14] B. Roffel, W.W. de Boer, "Analysis of power and frequency control requirements in view of increased decentralized production and market liberalization", Control Eng/ Pract., vol. 11, no. 4, pp. 367-375, 2003.

[15] A. Ulbig, T. S. Borsche, and G. Andersson, "Impact of low rotational inertia on power system stability and operation," in *IFAC World Congress*, vol. 19, no. 1, 2014, pp. 7290-7297.

[16] P. Ashton, C. Saunders, G. Taylor, A. Carter, and M. Bradley, "Inertia estimation of the gb power system using synchrophasor measurements," *Power Systems, IEEE Transactions on*, vol. 30, no. 2, pp. 701-709, March 2015.

[17] D. Jones, "Estimation of power system parameters," *Power Systems, IEEE Transactions on*, vol. 19, no. 4, pp. 1980-1989, November 2004.

APPENDIX A: GRID PARAMETERS USED IN SIMULATION

This appendix gives a overview of the parameter values of the block diagrams in Fig. 3. If necessary, parts of the block diagram are expressed in more detail. All parameters are normalized so that power is expressed in GW.

- The first order transfer function $M(s)$ depends on the grid parameters Inertia J and damping constant D of the control area (A.1). In this study the value D, expresses the change of load power for a frequency change of 1Hz. In the Dutch power system 1-2% of the load is frequency sensitive [3]. For the value D in (A.1), the assumption is made that 1.5% of the average load of the first two weeks of September, P_{load} , is frequency sensitive. A frequency sensitive load, is a load whereby power depends of the frequency of the grid.

$$M(s) = \frac{1}{Js+D} \begin{cases} Gain \quad K_M = \frac{1}{D} = 2.79 \quad GW/Hz \\ time\ constant \quad \tau_M = \frac{J}{D} = 5.59 \ s \end{cases}, \qquad (A.1)$$

Total inertia [2]: $J = 2$ GWs/Hz,

Damping constant: $D = D(\%) \cdot \frac{P_{load_{avg}}}{50} = 0.358$ GW/Hz.

- A change in tie-line flow between control area 1 and 2 occurs when $\Delta f_{12} = \Delta f_1 - \Delta f_2 \neq 0$. This is expressed by the following equation [2]: $\Delta P_{12} = \frac{2\pi\tau_{12}}{s} \cdot \Delta f_{12}$ with tie-line coefficient $\tau_{12} = 0.3$ GW/rad.
- The BRP, as described in Fig. 3, has two plants into service namely a non-reheat (A.3) and reheat (A.2) plant. Both plants are responsible for 50% of the momentary conventional production as defined in (A.4).

Reheat plant [3]: $G_1(s) = \frac{1}{(0.2s+1)} \frac{1.5s+1}{(0.3s+1)(5s+1)}$, (A.2)

Non reheat plant [3]: $G_2(s) = \frac{1}{(0.3s+1)} \frac{1}{(0.05s+1)}$, (A.3)

$P_{conventional}(t) = P_{market}(t) + P_{secondary}(t) - P_{wind}(t)$. (A.4)

- In Fig. 3 only the reheat plant $G_1(s)$ is responsible for the primary control action, represent as proportional gain K_p. The gain $K_p = 2.85\ GW/Hz$, which depends of the droop and nominal power of plant $G_1(s)$. In [14] the formula of K_p is defined. A typical value for the droop is 5% [14], this means a frequency change of 2.5Hz results in a 100% change of the produced power by plant $G_1(s)$.
- The secondary controller is shown in Fig. A.1 [3],[14]. The signals Δf_1 and ΔP_{12} are measured and used to construct the area control error (ACE) signal (A.5). The ACE signal is a measure of the power imbalance in the area. The relation between Δf_1 and power is displayed by the bias factor β. The bias factor (A.6) is a fixed value for all load levels and is recalculated every year [2].

$$ACE(t) = \beta \Delta f_1(t) + \Delta P_{12}(t) \qquad (A.5)$$

$$\beta = 0.1 * (K_p + D) = 0.32 \text{ GW/Hz} \qquad (A.6)$$

The ACE signal enters a Low pass filter, with time constant of 16 seconds, to avoid fast random variations. A smooth, robust and reliable control is preferable instead the ACE signal is rapid back to zero. This is to avoid unnecessary wear to the plants. The integrated filtered ACE signal is proportional allocated over all BRPs every four seconds. So, the participation factor in Fig. A.1 $\alpha_1 = \alpha_2 = \alpha_3$ and $\alpha_1 + \alpha_2 + \alpha_3 = 1$.

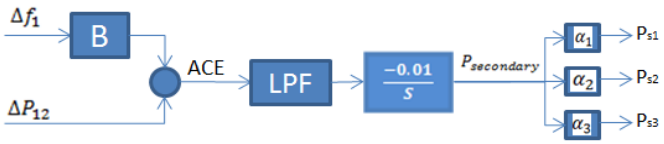

Fig. A.1 Schematic illustration of a secondary controller

APPENDIX B: ESTIMATION RESLUTS TWO CONNECTED AREAS

TABLE B.I

Identification results of block M(s) for two identical connected control areas, for the period 8-15 September 2009.

Day	J_{est}	D_{est}	F_{Db_VLoad}	F_{E_VLoad}	F_{J_VLoad}
Tue	2.02 (1.0%)	0.357 (0.3%)	[1 0]	[3 3]	[4 3]
Wed	1.99 (0.5%)	0.355 (0.8%)	[1 0]	[4 3]	[4 3]
Thu	2.00 (0.0%)	0.358 (0.0%)	[1 0]	[4 3]	[4 3]
Fri	2.02 (1.0%)	0.357 (0.3%)	[1 0]	[3 3]	[4 3]
Sat	2.00 (0.0%)	0.362 (1.1%)	[1 0]	[3 3]	[4 3]
Sun	2.04 (2.0%)	0.361 (0.8%)	[1 0]	[3 3]	[4 3]

APPENDIX C: ESTIMATION RESLUTS SELF-REGULATED AREA

TABLE C.I

Identification results of block M(s) for a self-regulated area, for the period 2-7 September 2009.

Day	J_{est}	D_{est}	F_{Db_VLoad}	F_{J_VLoad}
Tue	2.51 (25.5%)	0.344 (3.9%)	1	[3 2]
Wed	2.48 (24.0%)	0.351 (2.0%)	1	[3 2]
Thu	2.51 (25.5%)	0.344 (3.9%)	1	[3 2]
Fri	2.51 (25.5%)	0.344 (3.9%)	1	[3 2]
Sat	2.51 (25.5%)	0.344 (3.9%)	1	[3 2]
Sun	2.57 (28.5%)	0.337 (5.9%)	1	[2 1]

APPENDIX D: IDENTIFICATION FRAMEWOKR THREE CONNECTED AREAS

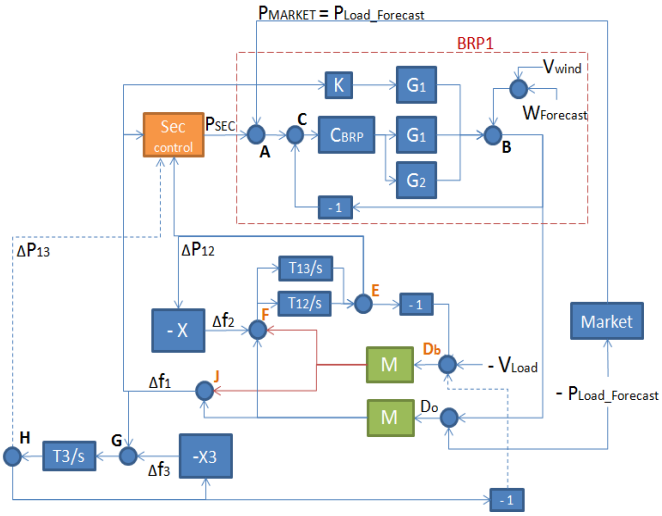

Fig. D.1: System identification framework for a control area which is connected to two neighboring control areas. There are two Tie-Line flows from control area 1 to area 2.